J. Inst. Eng. India Ser. B (April 2022) 103(2):293–304
https://doi.org/10.1007/s40031-021-00678-3

ORIGINAL CONTRIBUTION

A Cluster-Based Architecture for Three-Hop Communication in Next Generation Wireless Networks

P. Sree Harshitha[1] · P. S. S. Ganesh[1] · Chinmayi Nibhanupudi[2] · Hrishikesh Venkataraman[1]

Received: 10 January 2021 / Accepted: 8 September 2021 / Published online: 30 September 2021

Abstract Over the last 10 years, there has been an exponential growth of Internet services over cellular and wireless network. This has resulted in multiple wireless networks: macro-cell, micro-cell, femto-cell, legacy networks, etc. co-existing simultaneously. Multihop cellular networks have been well-investigated to support the heterogeneous wireless network scenario. However, this results in a very distributed and a non-optimum distribution of radio resources, leading to sub-optimal throughput of the network. Keeping this in mind, this paper proposes a three-hop heterogeneous wireless network architecture, wherein each hop would be from same network or other networks. Importantly, this paper proposes and provides a detailed analysis of a specific cluster-based architecture: *three-hop network*. This is the first instance where a three-hop architecture is analyzed. Accordingly, in every cell, three communicating pairs communicate using a given radio resource, but for only $1/3^{rd}$ the time slot period. This three-hop design enables a frequency reuse ratio of *one*. A comprehensive performance analysis indicates that the capacity obtained with a three-hop architecture is up to 20% higher than that can be obtained by two-hop architecture and 40% higher than traditional single-hop network. This is an extremely important result. It indicates the improvement that can be obtained in using specific design for multihop-based next generation LTE-advanced network.

Keywords Cellular wireless networks · Cluster-based design · System capacity · Three-hop

Introduction

Over the last few years, there has been a humongous increase in the data rate demand by the subscribers [1]. Notably, with the rapid success of viewing multimedia content over smart-phones, the requirement of high QoS (Quality of Service) and high QoE (Quality of Experience) has also increased manifold [2]. There exist inherent limitations in providing the requisite QoS and QoE through traditional single-hop cellular networks [3]. Particularly, in case of densely populated areas like city centers and shopping malls, subscribers tend to experience higher call blocking due to capacity limitations [4]. The solution is to interoperate between different macrocells (GSM, 4G) and small cells and have dynamic resource sharing between them. However, in case of stadiums, big malls, etc., where the number of subscribers can be in thousands and/or where the transmission power is reduced or not sufficient, it is not possible to reach large distances using single-hop communication. A technology that has evolved over the last decade is using the multihop communication for cellular wireless networks. In such an architecture, the communication between base stations (BSs) and mobile stations (MSs) could happen in multiple and varying number of hops, with varying and operator-controlled network technology across each hops [5]. Multihop communication techniques have the ability to extend the coverage of the network range indefinitely [6]. More

✉ Hrishikesh Venkataraman
hvraman@iiits.in

P. S. S. Ganesh
pavanganesh.pss@iiits.in

[1] Indian Institute of Information Technology (IIIT) Sri City, Chittoor 517646, India

[2] Indiana University–Purdue University, Indianapolis, USA

importantly, such a mechanism enables dynamic routing of information through intermediate nodes [7]. Many-a-times, this also results in a reduction in the transmission distance between BS and MS, which in-turn results in better received signal strength. Particularly, the reduced transmission power lowers the interference level and reduces the frequency reuse distance. More users can be accepted in the system when interference is less, thus resulting in increasing system capacity [8].

In the past 15 years, there has been considerable work on multihop cellular networks (MCN). An in-depth analysis on MCN's was done by Tam, *et.al* [4], in which they have identified and discussed the design decision factors and classified most of the existing MCN techniques. In fact, the work details about future research directions including the study of capacity and energy consumption and addresses design issues for MCNs such as cell size, routing and channel assignment. Having said that, available work in the literature focuses on two-hop design. The two-hop techniques include: *minimum relaying hop path loss*, *least total path loss*, *least maximum path loss*, etc. A time division multiple access mechanism is used whereby different hops communicate at different time instants in order to transfer the information from source to destination. A two-hop hierarchical wireless network using clustering mechanism was originally proposed by the authors in [9]. In the literature [9], the system capacity is observed using a clustering mechanism, and the capacity is 2.5 times higher than the cellular system which is using a single-hop mechanism. The authors of [10] proposed an intelligent time slot allocation mechanism for two-hop hierarchical wireless cellular network that is based on statistical multiplexing. Multihop clustering algorithms [11–13] were focused because it is the only way a set of mobile nodes can expand the borders beyond their communication range, thus allowing for better data aggregation and compression capacity. However, the mechanisms for optimum resource allocation were not considered in these papers.

A seminal work on optimal scheduling for multi-radio multihop cellular networks has modeled it as mixed integer programming problem and found it to be NP-hard [14]. In another work, the resource allocation in multihop cellular network has been modeled as *k*- Maximum Spanning Tree Problem and had been found NP-hard [15]. Moreover, the optimal radio resource allocation problem in multihop cellular networks, with the objective of throughput maximization is also proven to be NP-hard [16]. In order to find a quick-time solution, several heuristics have been proposed so far. These include: binary integer linear programming, tree-based allocation, etc [17]. A space-time graph based capacity evaluation of multihop cellular networks with opportunistic networking indicates that up to 73% capacity improvement can be obtained over conventional single-hop network [18]. However, their detailed analysis is again restricted to two-hops. Another piece of work investigates the use of genetic algorithms for optimal scheduling and routing for multihop cellular networks [19]. It does indicate that a good capacity can be achieved. However, the problem of such techniques is that they result in additional computation. Particularly, there is no literature on specific resource allocation techniques in three-hop networks.

On the other hand, a survey on different clustering algorithms for mobile ad-hoc networks was presented by Bentaleb *et.al* [20], wherein they introduced the important concepts for the design of algorithms for clustering. They also addressed a few important clustering problems with the network topology, routing, and algorithms for mobility. Notably, a work in the researches [21] presented several clustering algorithms for hierarchical communication and also explained their advantages and disadvantages based on few metrics like cluster stability, cluster overlapping and support for node mobility. The clustering mechanism for device-to-device (D2D) communications to carry out extremely dense RAN deployments which partially or completely mitigate the need for network operators was analyzed in the researches [22]. However, applying clustering solutions to D2D communication in multihop cellular design exponentially increases the number of clusters within a single cell.

With the suitable resource management techniques that are developed to enable multihop device-to-device communications, the spectral efficiency and energy efficiency can be improved [23]. Few such resource management algorithms in network-assisted multihop D2D scenarios are developed by [23]. The proposed approach, when integrated with a utility maximizing distributed PC scheme, can improve a system's throughput and energy efficiency. For a two-hop cellular network, a cluster-based architecture was proposed in the researches [24]. In the architecture proposed in the literature [24], any communication pairs' transmission distance is only half of the radius of the cell. In the proposed two-hop design, the radio resource is allotted to two communicating pairs in each cell at the same time, but only for half of the time duration. The important feature of this two-hop cluster-based design is that it allows a frequency reuse ratio of one. The two-hop cluster-based architecture was analyzed and tested with the real-world propagation parameters and a lognormal shadowing. The substantial improvement of the system capacity was observed using the cluster-based design. Notably, the capacity is 2.5 times more than that obtained using the traditional single-hop cellular system. However, to the best knowledge of the authors, there is no notable work on the cluster-based design beyond two-hop cellular networks. Moreover, with demand for data rates of 100 Mbps and

beyond in LTE and 5G systems, it is essential to investigate newer techniques that will support the same. Significantly, with improvement in parallel and distributed computing techniques, it is feasible to facilitate several parallel cluster-based computation, thereby supporting clustering over higher number of multiple hops.

In this work, a mixed three-hop hierarchical wireless network architecture is proposed such that the communication between the BSs and the MSs can be single-hop, double-hop or triple-hop mode. Notably, this work proposes a cluster-based design for a mixed three-hop cellular wireless network, wherein the maximum number of hops for communication between BS and any MS in the cell is limited to three hops. Particularly, it investigates an efficient design whereby the radio resources could be efficiently used among the three hops.

System Model

A cluster-based, three-hop cellular network was considered with BS at the center of the cell. The distance between the BS located at the center of the hexagonal cell and edge is the cell edge length, r. In the proposed three-hop cluster-based architecture, multiple clusters will be formed in every cell. Firstly, every cell is divided into three layers, i.e., single-hop layer, double-hop layer and triple-hop layers. The MSs located within $r/3$ communicate with the BS directly using single-hop. On the other hand, the MSs located between $r/3$ and $2r/3$ communicate with the BS in two-hops while those stationed beyond $2r/3$ from the BS communicate in three-hops. All MSs communicating in double-hop or triple-hop are first grouped into clusters. Given the hexagonal architecture, the double-hop region is divided into six clusters. As can be observed in Fig. 1, this would result in triple-hop region getting classified into 12 clusters.

1. Single Hop (SH) Layer: This region is contiguous to the BS and the data transfer between the BS and MS can be achieved through single-hop communication.
2. Double Hop (DH) Layer: This region is located between $r/3$ and $2r/3$. There will be two-hop communication between the MSs located in this region and BS. This region is further divided into several smaller areas called clusters, with a shape nearly that of an ellipse. The communication between MSs and BS within these clusters is through a cluster-head of the respective cluster. This is called as relay node or gateway node (GTW). This gateway node is represented by GTW_{m1n}, where m denotes the cell number, 1 denotes the first hop and n denotes the gateway node number. These GTWs are separated by $r/3$ from the BS, i.e., on the boundary adjoining single-hop layer and double-hop layer. Given that the length of the hexagonal edge is r, the maximum distance in double-hop layer between the GTW and the MSs will be equal to $r/3$. Therefore, the approximate transmission distance between BS and GTW_{m1n}, or between MS and GTW_{m1n} is $r/3$.
3. Triple-hop (TH) Layer: This region is located between $2r/3$ and r, i.e., around the double-hop layer. There will be three hop communication between MSs of TH layer and the BS. Further, this area also divided into smaller clusters. Similar to the BS-GTW communication at the double-hop layer, the MSs located in the clusters communicate to BS through gateway node. The gateway node of this layer is represented by GTW_{m2n}, where m denotes the cell number, 2 denotes the second hop and n denotes the gateway node number. These GTWs are separated by $2r/3$ from the BS. Hence, in the triple-hop layer, the distance from GTW to the MSs would be less than or equal to $r/3$. Therefore, the maximum separation between BS and GTW_{m1n}, between GTW_{m1n} and GTW_{m2n} and between MS and $GTW_{m2n}$is $r/3$.

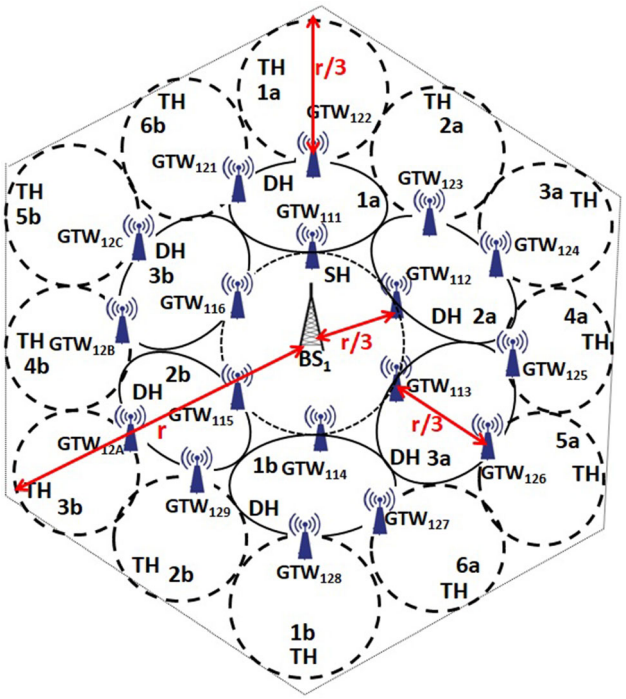

Fig. 1 Schematic view of a cluster-based three-hop cellular network

A single cell showing the schematics of a three-hop cellular architecture using clustering is shown in Fig. 2. For computational convenience, all clusters in the cell were considered to be circular. In each cell, there are six and twelve circular clusters in the DH and TH layers, respectively. For all clusters, a wireless terminal is chosen

as a gateway node, located at the boundary of the cluster's neighboring layers. The six GTW nodes in the DH layer are separated by $r/3$ from BS. Also, there are twelve GTW nodes located in the TH layer and the distance from GTW nodes of TH layer to GTW nodes of DH layer is $r/3$ and the distance from GTW nodes of TH layer to BS is $2r/3$. In the DH layer, gateways GTW_{m11} and GTW_{m14} are separated by a distance of $2r/3$ and considered diametrically opposite to each other. The same holds for the gateways GTW_{m12} and GTW_{m15}, and for GTW_{m13} and GTW_{m16}. Considering the TH layer, gateways GTW_{m21} and GTW_{m27} are separated by a distance of $4r/3$ and, diametrically opposite to each other. The same holds for the gateways GTW_{m22} and GTW_{m28}, GTW_{m23} and GTW_{m29}, GTW_{m24} and GTW_{m2A}, GTW_{m25} and GTW_{m2B}, and for GTW_{m26} and GTW_{m2C}. The GTWs may be fixed relay stations (RSs), mounted on some fixed locations like street lamps, or MSs, itself having data to transmit or receive. The fixed RSs would be at $r/3$ and $2r/3$ from BS for two hop and three hop, respectively. In a cellular network, the communication is typically divided into two modes - downlink and uplink. In this work, in order to ensure that the cluster-based architecture works in both modes, the analysis is divided into independent downlink and uplink mode as well.

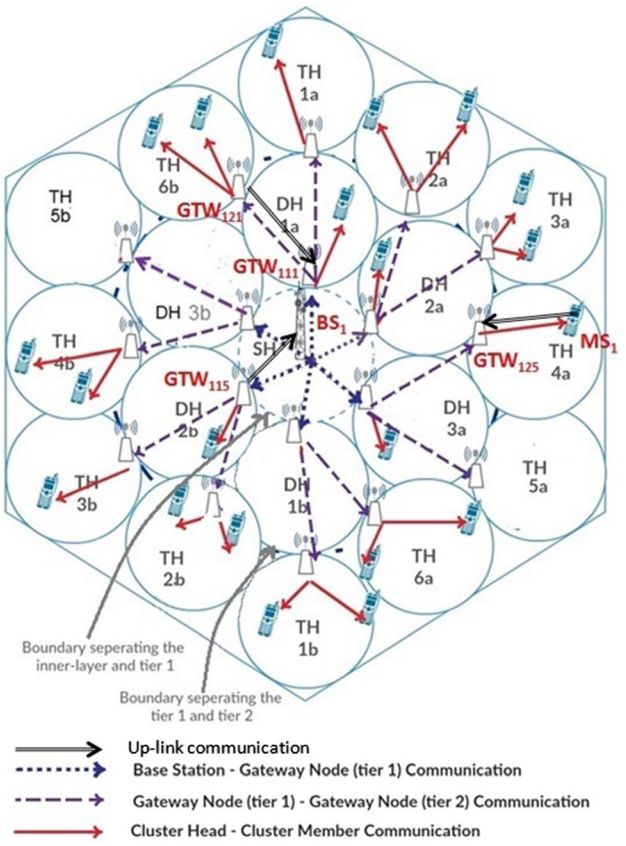

Fig. 2 Schematic model of the downlink and uplink in intracell three-hop cluster-based cellular communication

Downlink Mode

This section investigates and quantifies the intra-cell interference and inter-cell interference in the downlink mode.

Intracell Interference

The schematic model of the downlink of a three-hop cluster-based cellular network in a hexagonal cell is depicted in Fig. 2. The BS is located at the mid-point of hexagonal cell. The inner most cluster of the cell is the single-hop layer. Six gateway nodes (GTW_{m11}, GTW_{m12}, GTW_{m13}, GTW_{m14}, GTW_{m15}, GTW_{m16}) are present on the boundary adjoining the single-hop and double-hop region. Twelve gateway nodes - GTW_{m21}, GTW_{m22}, GTW_{m23}, GTW_{m24}, GTW_{m25}, GTW_{m26}, GTW_{m27}, GTW_{m28}, GTW_{m29}, GTW_{m2A}, GTW_{m2B}, GTW_{m2C} are present on the boundary adjoining the double-hop and triple-hop region. The MSs are assumed to be present in all the 19 clusters of the cell as shown in Fig. 2. Considering a three-hop downlink mode of communication, an example of intracell transceiver pairs communicate simultaneously are considered as shown in Fig. 2, and the communicating pairs are taken as:

- $BS_1 \longrightarrow GTW_{115}$
- $GTW_{111} \longrightarrow GTW_{121}$
- $GTW_{125} \longrightarrow MS_1$

In the considered communicating pairs, the downlink receiver where the over all interference experienced is GTW_{121}. For GTW_{121}, there will be intracell interference from BS_1 and GTW_{125}. To obtain the intracell interference at GTW_{121} caused by BS_1 and GTW_{125}, the distance between the downlink receiver and all transmitting stations is required. For calculating the intracell interference at GTW_{121} caused by BS_1, the distance is to be calculated. The maximum transmission distance from BS to GTW node of double-hop layer is $d = \frac{r}{3}$ and from GTW node of double-hop layer to GTW node of triple-hop layer is $d = \frac{r}{3}$; implying that the distance between the center of any cluster of the double-hop layer and GTW node of the respective cluster is $\frac{r}{6}$. The value of separation between BS_1 and GTW_{121} is found out to be eqn. (1) from Fig. 3(a). Similarly, the distance between two gateways GTW_{121} and GTW_{125} is obtained from Fig. 3(b). The distance from BS_1 to GTW_{125} and BS_1 and GTW_{121} is $r\sqrt{13}/6$. Moreover, the angle at BS_1 in the triangle having BS_1, GTW_{125} and GTW_{121} as edges is 120^0. By using the law of sines, distance between GTW_{125} and GTW_{121} is obtained, given in eqn. (2).

$$d_1 = \frac{r\sqrt{13}}{6} \tag{1}$$

$$d_2 = \frac{r\sqrt{13}}{2\sqrt{3}} \tag{2}$$

Inter-cell Interference

Since the cells in cellular networks are nearly hexagonal, each cell has six equidistant neighbors in its first tier [25]. From each of the six hexagonal adjacent cells, there will be three interferences at GTW_{121} node. The main cell is assumed to be $cell_1$ and numbering the six surrounding as $cell_2$, $cell_3$, $cell_4$, $cell_5$, $cell_6$ and $cell_7$, respectively, as shown in Fig. 4.

Considering three-hop downlink mode of communication, the inter-cell transceiver pairs from the horizontally adjacent cell 2 that communicate simultaneously are shown in Fig. 4:

- $BS_2 \longrightarrow GTW_{215}$
- $GTW_{211} \longrightarrow GTW_{221}$
- $GTW_{225} \longrightarrow MS_2$

It is observed that at the downlink receiver GTW_{121} node, there will be inter-cell interference from BS_2, GTW_{211} and GTW_{224} transmitters of $cell_2$. From hexagonal geometry, the distance between the centers of two adjoining hexagons whose radius is r is $d = r\sqrt{3}$. For calculating the inter-cell interference at GTW_{121} due to receiver GTW_{211}, the distance between the nodes is to be calculated. The value of separation between the nodes GTW_{211} and GTW_{121} is found out to be eqn. (3) from Fig. 5(a).

$$d_{GTW_{211}} = \frac{r\sqrt{43}}{2\sqrt{3}} \tag{3}$$

The distance between GTW_{121} and BS_2 can be found from eqn. (4) and is shown in Fig. 5(b).

$$d_{BS_2} = r\sqrt{\frac{121}{36} - \sqrt{\frac{13}{3}}cos(\theta)} \tag{4}$$

where θ is assumed to be the angle between the lines joining $GTW_{121} \longrightarrow BS_1$ and $BS_1 \longrightarrow BS_2$. Similarly, the distance from GTW_{225} to GTW_{121} is found from eqn. (5) and can be observed in Fig. 5(c).

$$d_{GTW_{225}} = r\sqrt{\frac{49}{12} - \sqrt{13}cos(\phi)} \tag{5}$$

where ϕ is assumed to be the angle between the lines joining $GTW_{121} \longrightarrow GTW_{125}$ and $GTW_{125} \longrightarrow GTW_{225}$.

On generalizing eqn. (3) for determining expression to find the separation distance between the receiver GTW_{121} and the transmitter GTW_{n11}, one obtains:

$$d_{GTW_{n11}} = r\sqrt{\frac{37}{12} - cos(120^\circ - 60i)} \tag{6}$$

where $i = 0 - 5$ for cell 2 to cell 7, respectively.

Similarly, on generalizing eqn. (4) for determining expression to find the separation distance between the receiver GTW_{121} and the transmitter BS_n, one obtains:

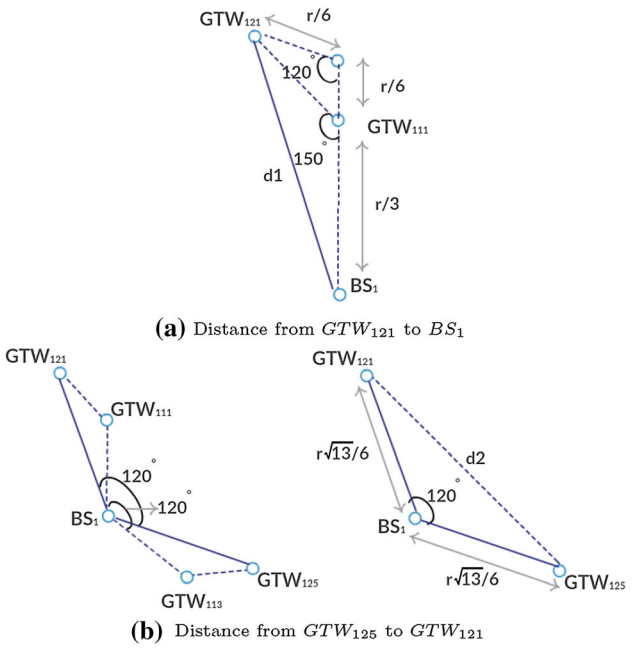

Fig. 3 Distance measurement for Interference from Intracell transmitters

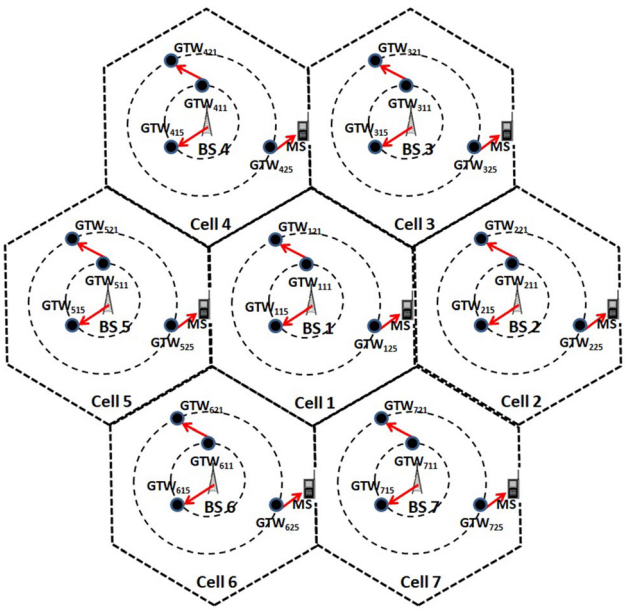

Fig. 4 Inter-cell Interference from center, tier-1 and tier-2 cells

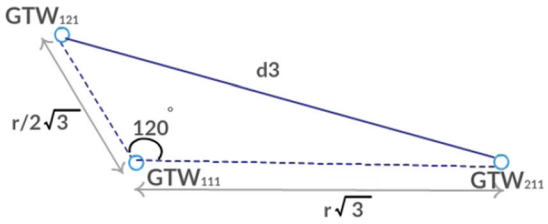

(a) Distance from GTW_{211} to GTW_{121}

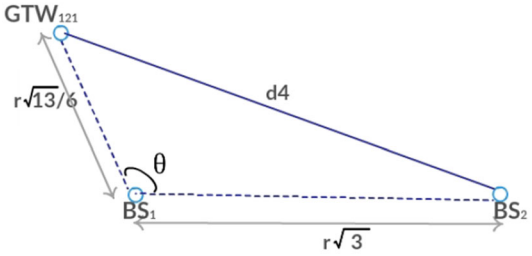

(b) Distance from BS_2 to GTW_{121}

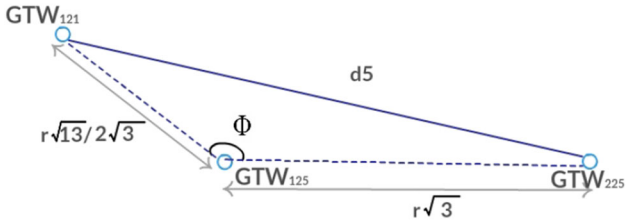

(c) Distance from GTW_{225} to GTW_{121}

Fig. 5 Distance measurement for interference from Cell-2 transmitters

$$d_{BS_n} = r\sqrt{\frac{121}{36} - \sqrt{\frac{13}{3}}cos(\theta - 60i)} \tag{7}$$

Likewise, on generalizing eqn. (5) for determining expression to find the separation distance between the receiver GTW_{121} and the transmitter GTW_{n25}, one obtains:

$$d_{GTW_{n25}} = r\sqrt{\frac{49}{12} - \sqrt{13}cos(\phi - 60i)} \tag{8}$$

β is used to represent the ratio between the calculated distance of the BS and GTW_{m1n} or GTW_{m1n} and GTW_{m2n} or GTW_{m2n} and MS, respectively, and the maximum transmission distance $d = r/3$. The expression of β for the $BS_1 \longrightarrow GTW_{115}$ link is as eqn. (9):

$$\beta_{BS_1} = \frac{d_{BS_1}}{d} = \frac{\sqrt{13}}{2} \tag{9}$$

Similarly, the expression of β for $GTW_{125} \longrightarrow MS_1$ link, $BS_n \longrightarrow GTW_{n15}$ link, $GTW_{n11} \longrightarrow GTW_{n21}$ link, $GTW_{n25} \longrightarrow MS_n$ link are represented in the eqns (10), (11), (12) and (13), respectively.

$$\beta_{GTW_{125}} = \frac{d_{GTW_{125}}}{d} = \frac{\sqrt{39}}{2} \tag{10}$$

$$\beta_{GTW_{n11}} = \frac{d_{GTW_{n11}}}{d} = 3\sqrt{\frac{37}{12} - cos(120° - 60i)} \tag{11}$$

$$\beta_{BS_n} = \frac{d_{BS_n}}{d} = 3\sqrt{\frac{121}{36} - \sqrt{\frac{13}{3}}cos(\theta - 60i)} \tag{12}$$

$$\beta_{GTW_{n25}} = \frac{d_{GTW_{n25}}}{d} = 3\sqrt{\frac{49}{12} - \sqrt{13}cos(\phi - 60i)} \tag{13}$$

For any communication pair in the downlink, the carrier-to-interference ratio (CIR) at the receiver is therefore given by eqn. (14).

$$\gamma = \frac{d_c^{-\alpha}}{d_{BS_1}^{-\alpha} + d_{GTW_{124}}^{-\alpha} + \sum_{n=2}^{7} d_{GTW_{n11}}^{-\alpha} + \sum_{n=2}^{7} d_{GTW_{n24}}^{-\alpha} + \sum_{n=2}^{7} d_{BS_i}^{-\alpha}} \tag{14}$$

The simplified equation of the CIR at the receiver for any communication pair is obtained after dividing the numerator and denominator by $d_c^{-\alpha}$ and is given in eqn. (15).

$$\gamma = \frac{1}{\beta_{BS_1}^{-\alpha} + \beta_{GTW_{124}}^{-\alpha} + \sum_{n=2}^{7} \beta_{GTW_{n11}}^{-\alpha} + \sum_{n=2}^{7} \beta_{GTW_{n24}}^{-\alpha} + \sum_{n=2}^{7} \beta_{BS_i}^{-\alpha}} \tag{15}$$

It can be clearly observed that the value of γ for any communication pair in the downlink is based on the relative location of the interfering transmitters. Moreover, it is also can be observed from eqn. (15) that the CIR is a function of the distance between two gateways; distance between a BS and a gateway; the number of clusters and the path loss exponent. Hence, the capacity of the system also varies significantly with the path loss exponent, number of clusters and the location of gateways.

Uplink Mode

This section details the intra-cell interference and inter-cell interference in uplink mode.

Intracell Interference

The schematic model of the uplink of a three-hop cluster-based cellular network in a hexagonal cell is similar to the one depicted in Fig. 2. Considering three-hop uplink mode of communication, the intracell transceiver pairs are:

- $GTW_{115} \longrightarrow BS_1$
- $GTW_{121} \longrightarrow GTW_{111}$
- $MS_1 \longrightarrow GTW_{125}$

The uplink receiver where the over all interference is calculated is GTW_{111}. For this receiver, there will be intracell interference from GTW_{115} and MS_1. As discussed earlier, the maximum transmission distance from BS to GTW node of double-hop layer is $d = \frac{r}{3}$ and from GTW node of double-hop layer to GTW node of triple-hop layer is $d = \frac{r}{3}$ implying that the distance between the center of any cluster of the double-hop layer and GTW node of the respective cluster is $\frac{r}{6}$. For calculating the intracell interference at GTW_{111} caused by GTW_{115}, the distance is to be calculated. The value of separation between GTW_{115} and GTW_{111} is found out to be eqn. (16) from Fig. 6(a).

$$d_3 = \frac{r}{\sqrt{3}} \tag{16}$$

Similarly, the distance between MS_1 and GTW_{111} is found out to be eqn. (17) from Fig. 6(b).

$$d_4 = \frac{r\sqrt{4-\sqrt{3}}}{3} \tag{17}$$

This distance is obtained with the assumption that MS_1 is on the same line as GTW_{113} and GTW_{125}

Inter-cell Interference

In each of the six hexagonal adjacent cells, there will be 3 interferences at GTW_{111} node. The main cell is assumed to be cell_1 and numbering the six surrounding as cell_2, cell_3, cell_4, cell_5, cell_6 and cell_7, respectively, as shown in Fig. 4. Considering three-hop uplink mode of communication, the

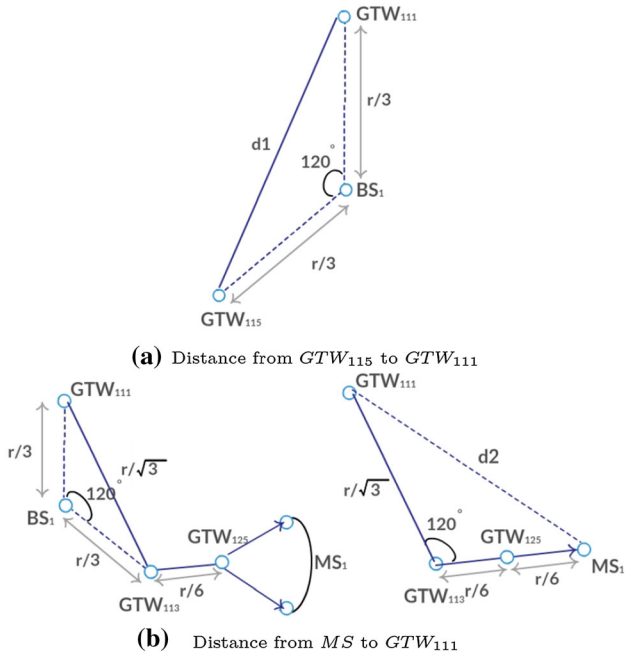

Fig. 6 Distance measurements for interference from Intracell receivers

inter-cell transceiver pairs from the horizontally adjacent cell_2 that are assumed to be communicating simultaneously, as shown in Fig. 4.

- $GTW_{221} \longrightarrow GTW_{211}$
- $GTW_{215} \longrightarrow BS_2$
- $MS_2 \longrightarrow GTW_{225}$

It is observed that at the uplink receiver GTW_{111} node, there will be inter-cell interference from GTW_{215}, GTW_{221} and MS_2 transmitters of cell_2. From hexagonal geometry, the distance between the centers of two adjoining hexagons whose radius is r is $d = r\sqrt{3}$. For calculating the inter-cell interference at GTW_{111} due to receiver GTW_{221}, the distance between the nodes is to be calculated. The value of separation between the nodes GTW_{221} and GTW_{111} is found out to be eqn. (18) from Fig. 7(a).

$$d_{GTW_{221}} = \frac{r\sqrt{31}}{2\sqrt{3}} \tag{18}$$

The distance between GTW_{215} and GTW_{111} is found out to be eqn. (19) from Fig. 7(b).

$$d_{GTW_{215}} = r\sqrt{\frac{10}{3} - 2cos(\delta)} \tag{19}$$

where δ is assumed to be the angle between the lines joining $GTW_{115} \longrightarrow GTW_{111}$ and $GTW_{115} \longrightarrow GTW_{215}$.

Similarly, the distance from MS_2 to GTW_{111} is found to be eqn. (20) from Fig. 7(c)

$$d_{MS_2} = r\sqrt{\frac{31}{9} - \frac{\sqrt{3}}{9} - \frac{2\sqrt{4-\sqrt{3}}}{\sqrt{3}}cos(\lambda)} \tag{20}$$

where λ is assumed to be the angle between the lines joining $GTW_{111} \longrightarrow MS_1$ and $MS_1 \longrightarrow MS_2$. On generalizing eqn. (18) for determining expression to find the separation distance between the receiver GTW_{111} and the transmitter GTW_{n21}, one obtains

$$d_{GTW_{n21}} = r\sqrt{\frac{37}{12} - cos60^\circ(i+1)} \tag{21}$$

Similarly, on generalizing eqn. (19) for determining expression to find the separation distance between the receiver GTW_{111} and the transmitter GTW_{n15}, one obtains eqn. (22).

$$d_{GTW_{n15}} = r\sqrt{\frac{10}{3} - 2cos(\delta - 60i)} \tag{22}$$

Likewise, on generalizing eqn. (20) for determining expression to find the separation distance between the receiver GTW_{111} and the transmitter MS_n, eqn. (23) is obtained.

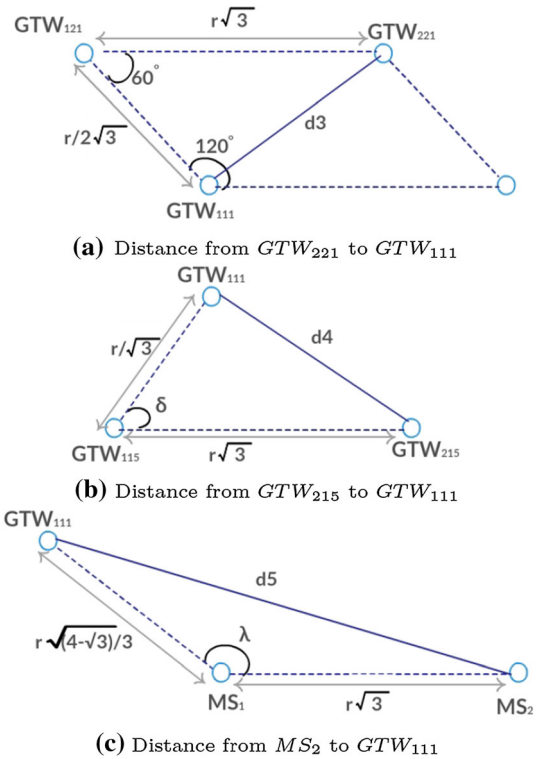

Fig. 7 Distance measurement for interferences from Cell-2 receivers

$$d_{MS_n} = r\sqrt{\frac{31}{9} - \frac{\sqrt{3}}{9} - \frac{2\sqrt{4-\sqrt{3}}}{\sqrt{3}}cos(\lambda - 60i)} \tag{23}$$

As discussed earlier, β is used to represent the ratio between the calculated distance of the BS and GTW_{m1n} or GTW_{m1n} and GTW_{m2n} or GTW_{m2n} and MS, respectively, and the maximum transmission distance $d = r/3$. The expression of β for the $GTW_{115} \longrightarrow BS_1$ link is as eqn. (24):

$$\beta_{GTW_{115}} = \frac{d_{GTW_{115}}}{d} = \sqrt{3} \tag{24}$$

Similarly, the expression of β for $MS_1 \longrightarrow GTW_{125}$ link, $GTW_{n15} \longrightarrow BS_n$ link, $GTW_{n21} \longrightarrow GTW_{n11}$ link, $MS_n \longrightarrow GTW_{n25}$ link are represented in eqns. (25), (26), (27) and (28), respectively.

$$\beta_{MS_1} = \frac{d_{MS}}{d} = \sqrt{4-\sqrt{3}} \tag{25}$$

$$\beta_{GTW_{n15}} = \frac{d_{GTW_{n15}}}{d} = 3\sqrt{\frac{10}{3} - 2cos(\delta - 60i)} \tag{26}$$

$$\beta_{GTW_{n21}} = \frac{d_{GTW_{n21}}}{d} = 3\sqrt{\frac{37}{12} - cos60(i+1)} \tag{27}$$

$$\beta_{MS_n} = \frac{d_{MS_n}}{d} = 3\sqrt{\frac{31}{9} - \frac{\sqrt{3}}{9} - \frac{2\sqrt{4-\sqrt{3}}}{\sqrt{3}}cos(\lambda - 60i)} \tag{28}$$

For any communication pair in the uplink mode, the CIR at the receiver is therefore given by eqn. (29).

$$\gamma = \frac{d_c^{-\alpha}}{d_{MS_1}^{-\alpha} + d_{GTW_{115}}^{-\alpha} + \sum_{n=2}^{7} d_{GTW_{n15}}^{-\alpha} + \sum_{n=2}^{7} d_{GTW_{n21}}^{-\alpha} + \sum_{n=2}^{7} d_{MS_n}^{-\alpha}} \tag{29}$$

The simplified equation of the CIR in uplink mode is obtained after dividing the numerator and denominator by $d_c^{-\alpha}$ and is given in eqn. (30).

$$\gamma = \frac{1}{\beta_{MS_1}^{-\alpha} + \beta_{GTW_{115}}^{-\alpha} + \sum_{n=2}^{7} \beta_{GTW_{n15}}^{-\alpha} + \sum_{n=2}^{7} \beta_{GTW_{n21}}^{-\alpha} + \sum_{n=2}^{7} \beta_{MS_n}^{-\alpha}} \tag{30}$$

As observed in the downlink mode, the value of γ for any communication pair in the uplink mode is also is based on the relative location of the interfering transmitters. Moreover, it is also can be observed from eqn. (30) that the CIR is a function of the distance between two gateways; distance between a gateway and MS; the number of clusters and the path loss exponent. Hence, the capacity of the system also varies significantly with the path loss exponent, number of clusters, location of the MS and the location of gateways.

Seven cells (till the first tier) as shown in Fig. 4 were considered for calculating the capacity in bps/Hz/cell, and the average of independent values was taken for system capacity. Every cell is surrounded in immediate vicinity by six cells. Similarly, there are twelve cells surrounding these six cells. Inter-cell interference in the first tier of cells was calculated using the traffic in the twelve 2^{nd} tier cells. Given that this second tier of cells is required to eliminate the boundary effects while calculating for the first tier of cells, the capacity for the twelve cells in the second tier was not calculated. There are three pairs transmitting at the same time in each of the seven cells. The value of γ at the receivers of those three communicating pairs is different and is based on the relative location of the interfering transmitters. The system capacity (of only the three-hop links) is therefore determined using the Shannon equation, given in eqn. (31).

$$C = \frac{1}{3N_c}\sum_{i=1}^{N_c}\sum_{j=1}^{N_l} log_2(\gamma_{ij} + 1) \tag{31}$$

Here, γ_{ij} represents CIR of the j^{th} pair communicating in the cell-i. The term N_l represents the number of simultaneously communicating pairs in the third layer of a single cell. For a three-hop cluster-based design, three pairs

communicate simultaneously, i.e., N_l = 3. The system capacity is calculated over 7 cells, i.e, N_c = 7. The average per-cell system capacity was obtained by summing up and averaging the Shannon capacity equation in eqn. (31) over all N_c cells.

Simulation Model and Results

A simulation model has been developed for the proposed cluster-based three-hop hierarchical cellular wireless network, and the simulations are carried out using MATLAB. Various locations such as an airport and shopping mall environment are considered for a coverage of 1 km^2. Within a coverage area of 1 km^2, there are 7 cells considered. The simulation parameters for the proposed architecture are given in Table 1.

For downlink mode, the value of θ lies between {90°, 150°} and the value of ϕ lies between {120°, 180°}. Hence, for an estimated γ value, the results are simulated across the path loss exponent (α) ranging from 2 to 4, by iterating across θ and ϕ for every degree. The results obtained by substituting these values in the downlink γ function w.r.t path loss exponent value are as shown in Fig. 8. The capacity is computed (in bps/Hz/cell) by substituting downlink SNR value in eqn. (31). The results obtained by substituting these values in the capacity downlink function w.r.t path loss exponent value are as shown in Fig. 9. It can be observed from Fig. 9 that across the path-loss variation from 2 to 4, the cluster-based three-hop design provides nearly 0.5 Mbps/Hz/cell increase in the capacity as compared to two-hop cluster-based design. This is a very significant observation which shows the potential improvement that can be achieved using three-hop mode. Further, the system capacity in downlink mode for three-hop and two-hop selection methods is shown in Fig. 10. The simulation results are plotted in the form of cdf (cumulative distribution function). It can be observed that the three-hop cluster-based design provides a consistent increase in the capacity of 0.5 bps/Hz/cell as compared to two-hop design.

For uplink mode, the value of λ lies between {120°, 180°} and the value of δ lies between {30°, 90°}. Hence, for an estimated γ value, the results are simulated across the path loss exponent (α) ranging from 2 to 4, by iterating across δ and λ for every degree. The results obtained by substituting these values in the uplink γ function w.r.t path loss exponent value are as shown in Fig. 11. It can be observed from Fig. 11 that for a path-loss exponent variation from $\alpha = 2$ to 3.5, the difference in signal-to-noise ratio between two-hop and three-hop mode is nearly always at 1 dB and this difference decreases to around 0.5 dB when α goes to 4. This shows the better signal reception in case of three-hop mode. Further, the capacity is computed by substituting the uplink SNR value in the uplink capacity equation. The results obtained by substituting these values in the capacity uplink function w.r.t path loss exponent value are as shown in Fig. 12.

As cumulative distribution function (cdf) gives the probability of achieving a required system capacity, the performance of the proposed architecture is observed using the cdf of the system capacity. Fig. 13 shows the cdf of the system capacity of the proposed three-hop selection method and the existing cluster-based two-hop architecture given in [24]; in uplink mode. It can be clearly observed from Fig. 13 that the system capacity obtained from the proposed three-hop cluster-base design is at least 0.5 Mbps/Hz/cell better than the existing cluster-based two-hop design. This implies that in the presence of moderate bandwidth of 100 KHz, a capacity improvement of around 500 Mbps can be obtained over two-hop design. This is a very significant result and shows the benefit that can be obtained using a three-hop design; in a single-cell.

Table 1 Simulation parameters

Parameter	Value
Coverage area	1 km^2
No. of cells (N_c)	7
No. of simultaneous communicating pairs (N_l)	3
Cell edge length (r)	200m (Approx)
Path loss exponent (α)	2 to 4
Cell shape	Hexagonal
Number of clusters per cell	19
Distance between a node and cluster head	$r/3$
Power distribution of each node	Uniform

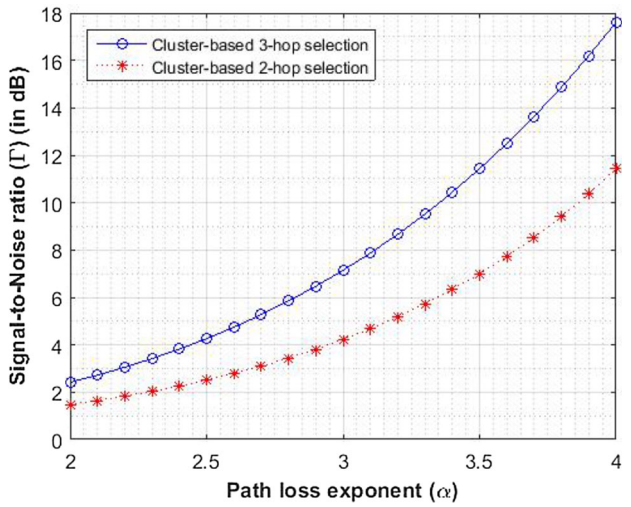

Fig. 8 Variation of γ with α variation in two hop [24] and proposed three-hop in downlink mode

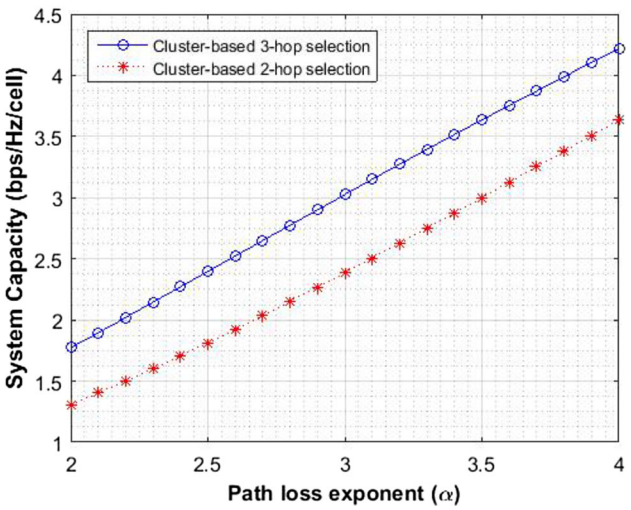

Fig. 9 System capacity with α variation for two hop [24] and proposed three-hop in downlink mode

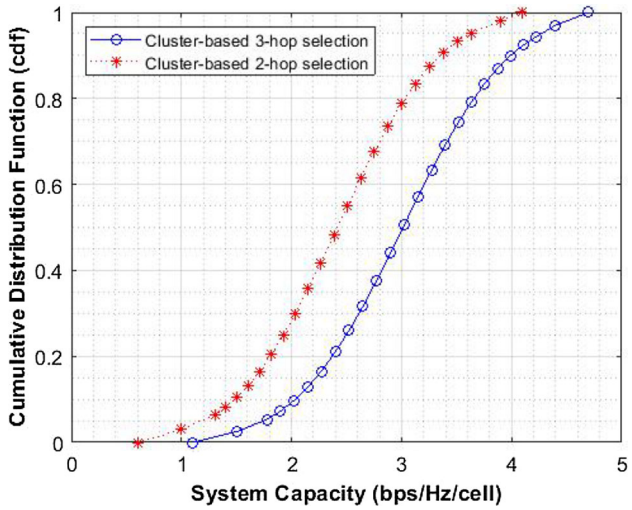

Fig. 10 cdf of the system capacity for two hop [24] and proposed three-hop in downlink mode

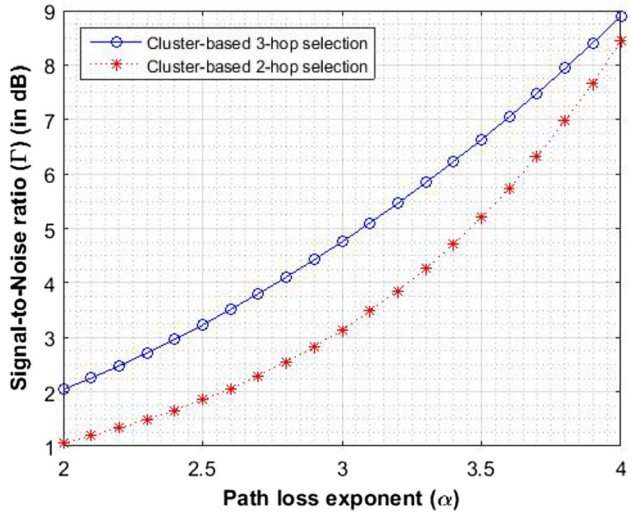

Fig. 11 Variation of γ with α variation in two hop [24] and proposed three-hop in uplink mode

Conclusions

This paper investigates an architecture for next generation multihop wireless network that would be useful in a device-to-device (D2D)/IoT oriented wireless cellular network. The emphasis is especially on the three-hop cellular wireless networks, in which a novel method for allocating resources has been proposed. The new scheme is designed using a technique of synchronized reuse of resources, known as cluster-based three-hop architecture. In the proposed architecture, each cell of the coverage area is classified into a single-hop layer, double-hop layer, and triple-hop layer. In the single-hop layer, the communication from MSs to BS is one hop; using a GTW terminal as relay node, communication from MSs in double-hop layer to the BS is two hops, whereas the MSs in the triple-hop layer use two GTW terminals on the path as relay nodes and communicate with the BS in three hops. This network model was designed using the interference avoidance model. This resulted in achieving both a frequency reuse ratio of *one* and also a higher spectral efficiency when compared to a state-of- the-art two-hop cellular network of up to 20%. An important point to note is that even though there is a three-hop communication, the proposed cluster-based design with synchronized resource reuse results in no additional overhead due to use of two intermediate relay/GTW nodes in transmitting information from source to destination. This

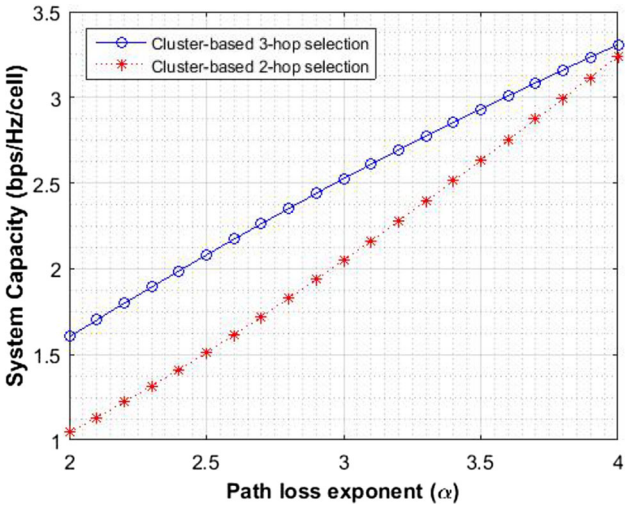

Fig. 12 Variation of system capacity with α variation for two hop [24] and proposed three-hop in uplink mode

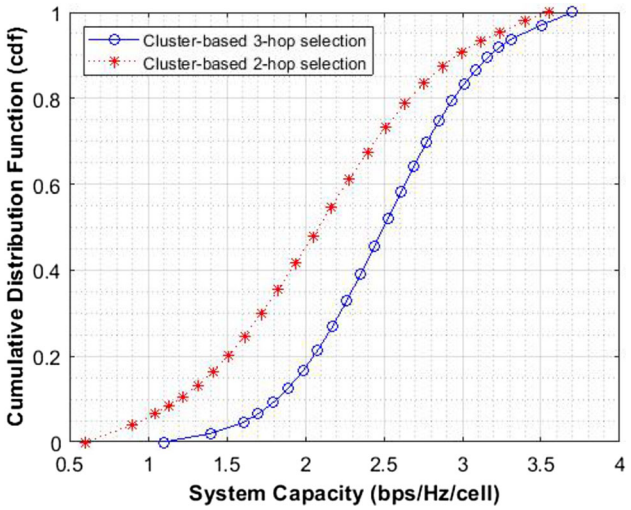

Fig. 13 cdf of the system capacity for two hop [24] and proposed three-hop in uplink mode

is the single-most benefit of a specific cluster-based architecture. Particularly, the increase in capacity is obtained without modifying the radio interface network model. It is specifically applicable to LTE and LTE-Ad networks where a multitude of IoT devices would result in multihop communication in cellular networks. Notably, the next step would be to use this analysis and develop a cluster-based design for generalized multihop network, which can provide a significantly higher capacity, that can eventually support tens and hundreds of Mbps data for each subscriber, over the next generation cellular network.

Acknowledgements The authors acknowledge the advise and technical support received from researchers in University of Edinburgh, UK and Dublin City University (DCU), Ireland.

Funding The authors declare that they have no known competing financial interests or personal relationships that could have appeared to influence the work reported in this paper.

Declarations

Conflict of Interest The authors declare that there is no conflict of interest regarding the publication of this paper.

References

1. D. Ebrahimi, H. Elbiaze, W. Ajib, "Device-to-device data transfer through multihop relay links underlaying cellular networks," *IEEE Trans. Veh. Technol.*, vol. 67, no. 10, pp. 9669–9680, oct 2018. [Online]. Available: https://doi.org/10.1109%2Ftvt.2018.2861391
2. L. Le, E. Hossain, "Multihop cellular networks: Potential gains, research challenges, and a resource allocation framework," *IEEE Commun. Mag.*, vol. 45, no. 9, pp. 66–73, sep 2007. [Online]. Available: https://doi.org/10.1109%2Fmcom.2007.4342859
3. Y. Miyahara, "Next-generation wireless technologies trends for ultra low energy," in *IEEE/ACM International Symposium on Low Power Electronics and Design*. IEEE, aug 2011. [Online]. Available: https://doi.org/10.1109%2Fislped.2011.5993661
4. Y. H. Tam, H. S. Hassanein, S. G. Akl, "A study of multi-hop cellular networks," *Wireless Commun. Mobile Comput.*, vol. 12, no. 12, pp. 1115–1129, nov 2012. [Online]. Available: https://doi.org/10.1002%2Fwcm.1041
5. F. S. Shaikh, R. Wismuller, "Routing in multi-hop cellular device-to-device (d2d) networks: A survey," *IEEE Commun. Surv. Tut.*, vol. 20, no. 4, pp. 2622–2657, 2018. [Online]. Available: https://doi.org/10.1109%2Fcomst.2018.2848108
6. I. Snigdh, N. Gupta, "Quality of service metrics in wireless sensor networks: a survey," *J. Inst. Eng. (India): Series B*, vol. 97, no. 1, pp. 91–96, dec 2014. [Online]. Available: https://doi.org/10.1007%2Fs40031-014-0160-6
7. G. Chen, J. Tang, J. P. Coon, "Optimal routing for multihop social-based d2d communications in the internet of things," *IEEE Internet Things J.*, vol. 5, no. 3, pp. 1880–1889, jun 2018. [Online]. Available: https://doi.org/10.1109%2Fjiot.2018.2817024
8. M. Arioua, Y. el Assari, I. Ez-zazi, A. el Oualkadi, "Multi-hop cluster based routing approach for wireless sensor networks," *Procedia Comput. Sci.*, vol. 83, pp. 584–591, 2016. [Online]. Available: https://doi.org/10.1016%2Fj.procs.2016.04.277
9. H. Venkataraman, G.-M. Muntean, "Dynamic time slot partitioning for multimedia transmission in two-hop cellular networks," *IEEE Trans. Mobile Comput.*, vol. 10, no. 4, pp. 532–543, apr 2011. [Online]. Available: https://doi.org/10.1109%2Ftmc.2010.170
10. H. Venkataraman, D. Gandhi, V. Tomar, "Multi-hop multi-band intelligent relay-based architecture for LTE-advanced multi-hop wireless cellular networks," *Wireless Pers. Commun.*, vol. 75, no. 1, pp. 131–153, aug 2014. [Online]. Available: https://doi.org/10.1007%2Fs11277-013-1352-0
11. V. Singh, H. Ochiai, "Performance analysis of the clustering-based multihop wireless energy harvesting sensor networks over symmetric and asymmetric fading channels," *Int. J. Distrib. Sens. Netw.*, vol. 13, no. 2, p. 155014771769384, feb 2017. [Online]. Available: https://doi.org/10.1177%2F1550147717693849
12. H. Shen, Z. Li, C. Qiu, "A distributed three-hop routing protocol to increase the capacity of hybrid wireless networks," *IEEE Trans. Mobile Comput.*, vol. 14, no. 10, pp. 1975–1991, oct 2015. [Online]. Available: https://doi.org/10.1109%2Ftmc.2015.2388476

13. K. Zheng, B. Fan, Z. Ma, G. Liu, X. Shen, W. Wang, "Multihop cellular networks toward LTE-advanced," *IEEE Veh. Technol. Mag.*, vol. 4, no. 3, pp. 40–47, sep 2009. [Online]. Available: https://doi.org/10.1109%2Fmvt.2009.933474
14. M. Li, S. Salinas, P. Li, X. Huang, Y. Fang, S. Glisic, "Optimal scheduling for multi-radio multi-channel multi-hop cognitive cellular networks," *IEEE Trans. Mobile Comput.*, vol. 14, no. 1, pp. 139–154, jan 2015. [Online]. Available: https://doi.org/10.1109%2Ftmc.2014.2314107
15. J.-S. Huang, Y.-N. Lien, "Topology design for multihop cellular network," in *2017 19th Asia-Pacific Network Operations and Management Symposium (APNOMS)*. IEEE, sep 2017. [Online]. Available: https://doi.org/10.1109%2Fapnoms.2017.8094129
16. Y. Liu, R. Hoshyar, X. Yang, R. Tafazolli, "Integrated radio resource allocation for multihop cellular networks with fixed relay stations," *IEEE J. Select. Areas Commun.*, vol. 24, no. 11, pp. 2137–2146, nov 2006. [Online]. Available: https://doi.org/10.1109%2Fjsac.2006.881603
17. Y. Sun, M. Brazil, D. Thomas, S. Halgamuge, "The fast heuristic algorithms and post-processing techniques to design large and low-cost communication networks," *IEEE/ACM Tran. Netw.*, vol. 27, no. 1, pp. 375–388, feb 2019. [Online]. Available: https://doi.org/10.1109%2Ftnet.2018.2888864
18. B. Coll-Perales, J. Gozalvez, "On the capacity gain of multi-hop cellular networks with opportunistic networking and d2d: A space-time graph-based evaluation," *IEEE Wireless Commun. Lett.*, vol. 6, no. 6, pp. 762–765, dec 2017. [Online]. Available: https://doi.org/10.1109%2Flwc.2017.2739161
19. B. Lorenzo, S. Glisic, "Optimal routing and traffic scheduling for multihop cellular networks using genetic algorithm," *IEEE Trans. Mob. Comput.*, vol. 12, no. 11, pp. 2274–2288, nov 2013. [Online]. Available: https://doi.org/10.1109%2Ftmc.2012.204
20. A. Bentaleb, A. Boubetra, S. Harous, "Survey of clustering schemes in mobile ad hoc networks," *Commun. Netw.*, vol. 05, no. 02, pp. 8–14, 2013. [Online]. Available: https://doi.org/10.4236%2Fcn.2013.52b002
21. C. S. Nam, Y. S. Han, D. R. Shin, "Multi-hop routing-based optimization of the number of cluster-heads in wireless sensor networks," *Sensors*, vol. 11, no. 3, pp. 2875–2884, mar 2011. [Online]. Available: https://doi.org/10.3390%2Fs110302875
22. G. Kollias, F. Adelantado, C. Verikoukis, "Spectral efficient and energy aware clustering in cellular networks," *IEEE Trans. Veh. Technol.*, vol. 66, no. 10, pp. 9263–9274, oct 2017. [Online]. Available: https://doi.org/10.1109%2Ftvt.2017.2716387
23. J. M. B. da Silva, G. Fodor, T. F. Maciel, "Performance analysis of network-assisted two-hop d2d communications," in *2014 IEEE Globecom Workshops (GC Wkshps)*. IEEE, dec 2014. [Online]. Available: https://doi.org/10.1109%2Fglocomw.2014.7063572
24. H. Venkataraman, S. Sinanovic, H. Haas, "Cluster-based design for two-hop cellular networks," *Int'l J. Commun. Netw. Syst. Sci.*, vol. 01, no. 04, pp. 370–385, 2008. [Online]. Available: https://doi.org/10.4236%2Fijcns.2008.14045
25. H. Venkataraman, S. Nainwal, P. Shrivastava, "Optimum number of gateways for cluster-based two-hop cellular networks," *AEU - Int. J. Elect. Commun.*, vol. 64, no. 4, pp. 310–321, apr 2010. [Online]. Available: https://doi.org/10.1016%2Fj.aeue.2008.12.010